RSC Advances

REVIEW

View Article Online
View Journal | View Issue

Cite this: *RSC Adv.*, 2025, **15**, 26728

Graphene-based nanomaterials: mechanisms and potentials in the fight against multidrug resistant bacterial infections: a review

Jianling Huang, †[a] Dengke Zhang,†[a] Chenghua Zhu,†[b] Shijun Chen,[a] Yueyue Wang,[a] Kexing Han,[a] Shusheng Ci*[a] and Yunxiang Lv*[a]

Bacterial infections pose a serious threat to human health, and antibiotic resistance has greatly hindered their clinical application. Therefore, new antibacterial compounds or alternative approaches are urgently needed. In recent years, nanoscience and nanotechnology have developed a number of antimicrobial nanoparticles that can be used as new tools to fight deadly bacterial infections. Graphene-based nanomaterials (GBNs), such as graphene oxide (GO) and reduced graphene oxide (rGO), have shown great potential in the treatment and management of bacteria-induced infectious diseases due to their outstanding biological properties. This review provides a comprehensive understanding of the antibacterial application of GBNs *via* summarizing their classifications, structural features, antibacterial mechanisms and concrete applications in the treatment of multidrug resistant (MDR) bacterial infection. We highlight the advances in development of GBNs and GBNs-based treatment strategies, including photothermal therapy (PTT), photodynamic therapy (PDT) and multiple combination therapies. In addition, we conclude and discuss the challenges and problems in using these nanomaterials. Collectively, we believe that GBNs have the potential to be an effective clinical treatment for MDR bacterial infections.

Received 25th February 2025
Accepted 16th July 2025

DOI: 10.1039/d5ra01352f

rsc.li/rsc-advances

1. Introduction

The situation in clinical microbiology has changed drastically over the last decades. The wide use of broad-spectrum antibiotics unavoidably leads to the emergence of antibiotic-resistant bacterial strains which threatens public health globally. Statistical results show that 700 000 people worldwide die from antibiotic-resistant bacteria annually,[1] and some experts indicate that number might rise to 10 million by 2050 which would exceed that caused by cancer. Drug-resistant bacteria could fight antibiotics in complex channels, such as the formation of biofilm, decreased cell permeability, inactivated enzyme production like metallo-β-lactamase (MBL), target mutation, and increased efflux.[2–4] Among them, bacterial biofilm plays a crucial role in drug resistance which brings great difficulties for clinical treatment of infectious disease. The bacterial biofilm not only enhances the tolerance to robust attack from microenvironment and immune system, but also prevents antibiotics from penetrating into bacteria so that reduce efficacy of antibiotics. In addition, bacterial biofilm is able to induce chronic and recurrent infection which prolongs antibiotic therapy, and then resulting in increased drug side effects.[5] In order to solve the urgent crisis of antibiotic resistance, new antibiotics need to be discovered constantly. However, some factors limit the development of novel antimicrobials, such as long-time consuming, large cost and faster emergence of new drug resistance than new antibiotics.[6] Many pharmaceutical companies are reluctant to develop antimicrobial agents because they consider the market for new antibiotics is small, and might not sell enough medicines to remedy their costs. Therefore, it is essential to exploit alternate antibiotic-independent approaches to combat multidrug-resistant (MDR) bacteria.

In recent years, nanotechnology has provided a new insight into the diagnosis and treatment of infectious disease. Nanomaterials are supposed to be an effective supplement to overcome MDR bacteria due to their different antibacterial mechanisms from traditional antibiotics.[7] Firstly, nanomaterials can directly destroy the bacterial membrane and interact with DNA and proteins to obstruct proper functioning of cellular machinery. Secondly, nanomaterials can execute multiple bactericidal pathways, making it difficult for bacteria to adapt to these therapeutics. Thirdly, they could indirectly damage microbial cell components and viruses through producing reactive oxygen species (ROS).[8]

[a]*Department of Pulmonary and Critical Care Medicine, The First Affiliated Hospital of Bengbu Medical University, Bengbu, Anhui, 233000, China. E-mail: yunxianglv@126.com*
[b]*Nanjing Pukou Hospital of TCM, Pukou Hospital of Chinese Medicine Affiliated to China Pharmaceutical University, Nanjing 210000, China. E-mail: zhuchenghuacheng@163.com*
† Co-first authors.

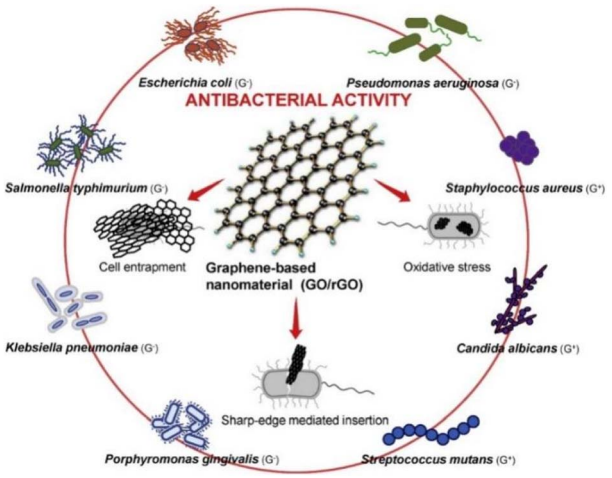

Fig. 1 Multiple antibacterial mechanisms of graphene-based nanomaterials against various pathogens. Reproduced with permission.[12] Copyright 2018, Elsevier.

Moreover, nanomaterials have been used as excellent antimicrobial delivery vehicles which can selectively transport drugs to the infection site and increase their retention time in blood.[9]

Graphene, obtained for the first time through micromechanical exfoliation of graphite in 2004, is a two-dimensional (2D) layer of sp^2-hybridized carbon atoms located in a honeycomb lattice. Graphene-based antibacterial nanomaterials (GBNs), including graphene oxide (GO), reduced graphene oxide (rGO), graphene quantum dots (GQDs), graphite and graphite oxide have various derivatives with different properties and functions, such as high mechanical strength, excellent electrical conductivity, wide surface area, zero band gap width, excellent electrical, thermal conductivity and biocompatibility.[10] Recent years, GBNs have found application in many fields, such as antibacterial action, pathogens bio detection, cancer therapy and drug and gene delivery. GBNs can fight against Gram-positive and Gram-negative bacteria and even fungal pathogens. Fig. 1 showed some of the representative bacteria. Among the various GBNs, GO showed the highest antibacterial activity, followed by rGO, graphite and graphite oxide.[11]

In this review, we focus on the recent advances in the design of GBNs for applications in multidrug resistant bacterial infection detection and treatment, which aims to provide a guidance for subsequent research and clinical treatments.

Table 1 The antibacterial effect of graphene nanomaterials[a]

				Antibacterial efficacy		
Materials	Combined therapy	Loading drugs	Bacterial species	Parameter	Value	Ref.
GO	—		Kp	IR (%)	>95%	16
			MRSA		64.3%	
Go-Ag	PTT		MDR *E. coli*	IR (%)	>96%	17
TOB-GO-Ag	PDT	Tobramycin	*E. coli*	IR (%)	Nearly 100%	18
GQDs-BC	—		MASA	MIC	200	19
N-GQDs	PDT		MASA	IR (%)	>97%	20
GOD	PDT/PTT		MASA	IR (%)	100%	21
rGO-Fe_2O_3			MRSA	ZOI (mm)	18 ± 0.25	22
			VRSA		16 ± 0.65	
			CRSA		18 ± 0.16	
GO-Ag HN			CRPA	IR (%)	Most	23
rGO/Ag	PTT		Ab, Kp and PA	IR (%)	97.6	24
TG-NO-B	PTT + NO		Ab, Kp and PA	IR (%)	55.6 ± 9.0, 55.2 ± 9.5 and 55.6 ± 9.0	25
GO-NTA-Ce	PTT		MRSA	IR (%)	99.9	26
GO-CS/ZnO		Tetracycline	MDR PA	IR (%)	100	27
SGQDs-CORM@HA	PDT + CO		MRSA	IR (%)	100	28
GrZnO-NCs		Curcumin	MRSA	ZOI (mm)	14.6 ± 2	29
GO/CS/Cu-POM			KR *E. coli*	IR (%)	99.93	30
			AR *E. coli*		97.94	
rGO/AuNS	PDT		MRSA	IR (%)	68	31
rGO-IONP	PTT		MRSA	IR (%)	81	32
Eu-Van-rGO	PTT		KR *E. coli*, OR *S. aureus*	IR (%)	100	33
					>3	
NGO-BSA-AIE	PTT		AMO-resistant *E. coli*	IR (%)	>99%	34
	PDT					
GAGO			MRSA MRSA-pvl+	MIC	100	35
			and MRSA-pvl−		150	
					150	

[a] Abbreviation: MRSA, methicillin resistant *Staphylococcus aureus*; KP: *Klebsiella pneumoniae*; PA: *P. aeruginosa*; VRSA: vancomycin-resistant *S. aureus*; CRSA: ciprofloxacin-resistant *S. aureus*; CRPA: carbapenem-resistant PA; KR: kanamycin resistant; AR: ampicillin resistant; AMO: amoxicillin; OR: oxacillin resistant; ZOI: zone of inhibition (mm); MIC: minimum inhibitory concentration (μg mL^{-1}); GA: gallic acid; IR: inhibition rate.

Table 1 reveals the GBNs with antibacterial activity against different MDR and biofilm-associated pathogens.

2. Classification and their unique properties

2.1. Graphene oxide (GO)

GO is a typical two-dimensional crystal structure with oxygen functional groups and single atomic layer. This layer is composed of sp^2 and sp^3 carbon atoms arranged in a hexagonal grid as its basic skeleton, rendering GO with large surface area and hydrophobic nature.[13] Oxygen groups such as hydroxyl groups, carbonyl groups, and epoxy groups are distributed on basal planes and edges of the skeleton.[14] Distinctive nanosheets and oxygen-containing groups confer GO not only a great hydrophilicity and dispersity in aqueous solutions, but also the great antibacterial potentials *via* multiple mechanisms.[15] GO is derived from graphite by various oxidation strategies, the most commonly employed of which is the improved Hummers' method.[14] Although GO derived from different synthesis methods is basically consistent, they are prone to have some differences in certain aspects or properties such as lateral dimensions and the number of oxygen functional groups. A variety of graphene derivatives have been synthesized based on GO functionalized with abundant functional groups such as brominated graphene (rGO-Br) and aminated graphene (rGO-Am). Amine is known to be an electron-absorbing group, and functionalization of graphene with amine can modify its electronic structure, particularly to improve electrical conductivity and provide controllable work function engineering.[36] Aminated graphene has excellent applications in photovoltaics, gas sensing and biosensing, drug delivery, and composite material formation.[37,38] TEM images (Fig. 2) demonstrate the morphology of the initial GO, rGO-Br, and rGO-Am. No rips or nanoscale holes are observed in the initial GO (Fig. 2a). After bromination, rGO-Br exhibits a lamellar defect-free structure and can be distinguished as a monolayer platelet (Fig. 2b). The amination preserved a good crystalline structure with long-range order up to tens of nanometers. However, rGO-Am shows a tendency to roll and wrinkle the initially flat graphene monolayer platelets, leading to the formation of localized multilayer regions within a single rGO-Am platelet (Fig. 2c). ED patterns consist of distinguishable hexagonal diffraction patterns that rotate around each other (Fig. 2c).[36]

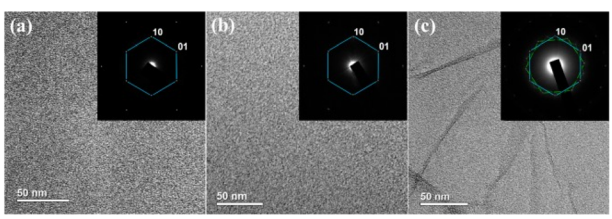

Fig. 2 TEM images and corresponding selective area electron diffraction (SAED) patterns of (a) the initial GO, (b) rGO-Br, (c) rGO-Am. Reproduced with open access under Creative Commons.[36] Copyright 2020, The Maxim K. Rabchinskii *et al.* Springer Nature.

2.2. Reduced graphene oxide (rGO)

rGO is the reduced form of GO and restores the conductivity and absorbance of graphene to some extent and is more hydrophobic than GO due to the reduction of the oxygen-containing groups.[37] Different from the sheet shape of GO, rGO is a circular particle with width obviously larger than height, which is attributed to enhanced hydrophobicity.[38] rGO is often obtained by reducing GO, including chemical reduction, electrochemical reduction and thermal reduction.[39] Among these methods, hydrothermal reduction seems to be the most convenient and environment-friendly approach since it only requires an autoclave with a Teflon-lined container along with a furnace. H. Huang *et al.*[40] elucidated the structural, morphological and electrical changes during the reduction process from the first 30 minutes to 10 hours at 200 °C. Before hydrothermal treatment, the GO samples showed a laminated structure (Fig. 3a). After dispersion in water, single or several layers of GO were obtained, with the thickness of a single layer being 0.8–0.9 nm (Fig. 3e). SEM and TEM images of rGO reduced for 1 h, 4 h, and 10 h were shown in Fig. 3(b–d) and (f–h). SEM images after 1 h reduction showed that rGO retained a layered structure, while TEM images revealed the coexistence of GO and rGO. The number of layers was reduced to less than 10 (Fig. 3f). As the reduction time increased, the layering became disordered, crumpled, and smaller. Compared to GO, rGO exhibited higher conductivity, better mechanical properties, and stronger photothermal effects, endowing it with significant potential for applications in photothermal therapy (PTT) against cancer and heat-induced controlled drug release.[41] Meanwhile, the photothermal effect of rGO can also play important roles in antibacterial use.[42]

2.3. Fluorinated graphene

Fluorinated graphene (FG) is a new class of two-dimensional materials formed by covalent bonding of carbon atoms and fluorine atoms in graphene. The introduction of fluorine atoms with the strongest electronegativity dramatically changes the electron distribution of graphene, leading to a series of unique changes in optical, electronic, magnetic, interfacial properties and so on. In addition, the fluorine atoms in FG have the unique property of improving dispersion and friction by increasing the

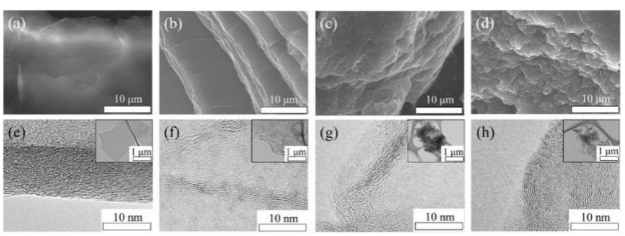

Fig. 3 SEM images of (a) GO, and its deoxygenated samples treated under (b) 1 h, (c) 4 h and (d) 10 h. The corresponding TEM images are shown in (e–h), respectively. The insets of TEM images showing the sheets in low magnification. Reproduced with open access under Creative Commons.[40] Copyright 2018, The H. Huang *et al.* Springer Nature.

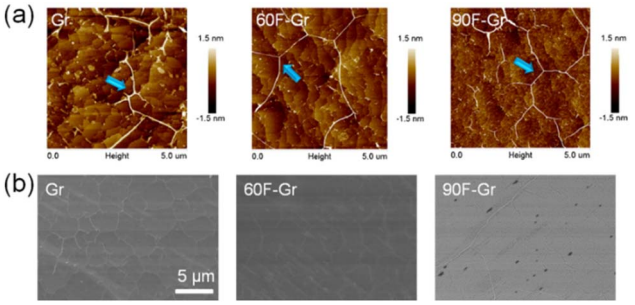

Fig. 4 AFM images (a) and SEM images (b) of graphene and fluorinated graphene with variable exposure time in the SF_6 atmosphere. Reproduced with permission.[46] Copyright 2018, Elsevier.

interlayer distance of graphene.[43] Various methods have been used to synthesize FG, including XeF_2 etching, plasma-assisted decomposition of CF_4, SF_6, or mechanical and chemical exfoliation of fluorographite.[44] From the AFM image of graphene in Fig. 4a, it appears that the distinct wrinkles (indicated by blue arrows) originating from the difference in thermal expansion coefficients between the Ge substrate and graphene are retained after fluorination. The SEM image in Fig. 4b shows that the surface morphology of partially fluorinated graphene is similar to that of the pristine graphene, while the fully fluorinated graphene is changed. The pale morphology of F–Gr implies poor electrical conductivity because of the small number of secondary electrons in the SEM measurements. Partially fluorinated graphene exhibited better antibacterial ability and cytocompatibility than pristine graphene and fluorinated graphene.[45]

2.4. Graphene quantum dots (GQDs)

GQD is a single layer of carbon atoms in a honeycomb structure with large surface area and excellent thermal/chemical stability.[47] GQD can be synthesized by various top-down and bottom-up approaches.[48] Scattered evidence show that GQDs themselves have no antibacterial property.[49] But GQDs have the characteristics of peroxidase or oxidase are able to transform H_2O_2 and $^3O_2$ into highly active molecules (such as OH radicals, $^1O_2$) under light irradiation. It is worth mentioning that GQD is capable of producing higher singlet oxygen yield (>1.3) compared to conventional photosensitizers (<1).[50] These properties endow GQDs to be a candidate for photodynamic therapy which can target and kill microbial pathogens even multi-drug resistant bacterial.[51] However, the special infection microenvironment of hypoxic and low H_2O_2 concentration limit the ROS efficiency. To enhance antimicrobial therapy, GQD could exert antibacterial function *via* modifying or combining with other materials, such as silver-based nanocomposite.[52]

3. Antibacterial mechanisms of graphene-based materials

Three main possible antimicrobial mechanisms of GBNs have been proposed as follows. (i) ROS mediated oxidative stress. Wu

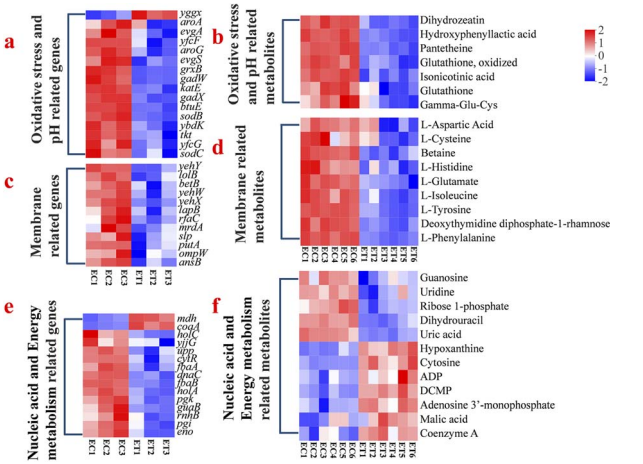

Fig. 5 Antibacterial mechanisms of N-GQDs. Differentially expressed genes and differential metabolites in *E. coli*. (a) Oxidative stress and pH related genes. (b) Oxidative stress and pH related metabolites. (c) Membrane related genes. (d) Membrane related metabolites. (e) Nucleic acid and energy metabolism related genes. (f) Nucleic acid metabolism and energy related metabolites. Reproduced with permission.[53] Copyright 2022, Elsevier.

et al.[53] demonstrated that N-GQDs produce ROS, which can destroy enzymes, catalases (CATs), glutathione (GSH) systems and non-enzymatic antioxidants (vitamin E, ascorbic acid, *etc.*) in *E. coli* when exposed to solar irradiation. As shown in Fig. 5a, 12 differentially expressed genes (*yggX*, *btuE*, *grxB*, *sodB*, *katE*, *yfcG*, *yfcF*, *sodC*, *ybdK*, *aroG*, *aroA*, and *tkt*) were found to be related to oxidative stress in *E. coli* after N-GQD treatment. Importantly, the up-regulation of the *yggX* gene suggested that the N-GQDs could cause oxidative stress in *E. coli*. In addition, down-regulated *yfcG* and *ybdK* genes associated with the GSH antioxidant system resulted in decreased levels of γ-glutamylcysteine, GSH and oxidized glutathione (GSSG), respectively, in *E. coli* (Fig. 5b). As known, GSH is an important reductase in bacteria, and its level can reflect the accurate extent of oxidative stress. Therefore, it is believed that GBNs induced ROS is the driver of bacterial oxidative stress. (ii) Nano knife effect: graphene material can be inserted into the cell membrane, destroying the phospholipid bilayer and thereby disrupting the cell membrane structure. This mechanism is particularly relevant for certain types of GBNs that exhibit sharp edges or flakes, which can physically pierce the cell membrane.[54] In addition to membrane disruption, some GBNs, such as N-GQDs, have been shown to inhibit cell wall synthesis by down-regulating the expression of genes involved in cell wall component synthesis (*e.g.*, *slp*, *lolB*, *lapB*, *rfaC*, *mrdA*, *ansB*, and *ptuA* in *E. coli* (Fig. 5c).[53] (iii) Wrapping or trapping the bacteria, and limiting physical movements and metabolism of bacteria. Cell entrapment is recognized as an important antibacterial mechanism which describes the bacterial cells trapped by GBNs sheets upon their direct physical contact. Trapped bacteria are isolated from the external environment and their access to nutrients is restricted. The trapping effect only temporarily inhibits the growth of the bacteria but does not kill them. Perreault *et al.* found that bacteria trapped by Go sheets lost their viability but

could regain their proliferation capacity after isolation by sonication.[55] GBNs also interfere with bacterial nucleic acid synthesis and energy metabolism. For example, N-GQD interferes with DNA semiconservative replication, pyrimidine metabolism and purine metabolism through down-regulating the genes involved in the replication of DNA, such as the *dnaC*, *holC*, *holA*, *rnhB*, *cytR*, *upp*, *guaB*, and *yjjG*. Down-regulation of the expression of *AroA*, *ansB* and *ptuA* may lead to a decrease in the production of natural osmoregulators such as L-isoleucine, L-phenylalanine, L-cysteine, L-histidine, L-aspartate, L-tyrosine and L-glutamate (Fig. 5d and e). N-GQDs interfere with bacterial energy metabolism by blocking the glycolytic pathway, tricarboxylic acid (TCA) cycle and oxidative phosphorylation, leading to the accumulation of cytidine-5′-monophosphate (CMP), deoxycytidine monophosphate (dCMP), cytosine, adenosine 5′-monophosphate (AMP), adenosine 5′-diphosphate (ADP) and hypoxanthine (Fig. 5f).[53]

4. Factors affecting antibacterial effect

Antibacterial efficacy of nanoparticles is correlated with the structural and physical properties such as size, shape, surface charge, concentration, and colloidal state.[56] For instance, the antibacterial activity of GO sheets was dependent on lateral size, and larger GO showed stronger antibacterial activity than that of small, which is due to the easy coating on the surface of bacteria, thus damaging their cellular integrity.[57] In addition, the dissociation state and content of oxygen-containing functional groups play an important role in the antimicrobial properties. These functional groups not only contribute to the negative surface charge of GBNs, enhancing electrostatic interactions with positively charged bacterial cell membranes and inhibiting bacterial adhesion through electrostatic repulsion, but also participate in redox reactions to generate ROS, leading to bacterial cell death.[58,59] Furthermore, the antibacterial activity of GBNs is related to the physiological state of cells for both Gram-negative and -positive bacteria. The order of GO susceptibility of *E. coli* to GO with respect to the growth phases (exponential $\gg$ decline > stability) which associates well with the changes in membrane ultrastructure of the cells.[50]

5. Therapeutic applications

5.1. As independent antibacterial agents

Nanomaterials, leveraging their unique physio-chemical properties, offer a promising strategy to circumvent antibiotic-resistance mechanisms by activating multiple novel bactericidal pathways, thereby achieving robust antimicrobial activity.[60–62] GBNs have a broad antibacterial spectrum and exhibit toxicity to both Gram-positive and Gram-negative bacteria.[54,63] Furthermore, the antibacterial action of GBNs primarily hinges on physical mechanisms, which are fundamentally distinct from the molecular-level mechanisms by which traditional antibiotics operate. Consequently, bacteria are considerably less likely to develop resistance to graphene derivatives. However, most of these studies have demonstrated the antibacterial activity of GBNs *in vitro* using model bacteria. For example, Zmejkoski[19] constructed a novel hydrogel composite (GQDs-BC) composed of bacterial cellulose (BC) and graphene quantum dots (GQDs) for wound healing treatment. GQDs-BC showed significant inhibition effect towards *Staphylococcus aureus* and *Streptococcus agalactiae* and bactericidal effect towards MRSA, *E. coli*, and PA in a dose-dependence manner. GQDs-BC inhibited the bacteria growth at a concentration of 0.2 mg mL^{-1}, and killed bacteria at a concentration of 2 mg mL^{-1}. While Xu Wu *et al.*[64] investigated the antimicrobial properties of graphene oxide (GO) both *in vitro* and *in vivo*. Their findings revealed that GO effectively inhibited and eradicated the growth and dissemination of MDR *Klebsiella pneumoniae* (Kp). This treatment significantly enhanced cell survival rates, minimized tissue damage, alleviated inflammatory responses, and prolonged the survival of the mice with pneumonia. Mechanically, GO decreased polymorph nuclear neutrophil (PMN) penetration, the generation of ROS in alveolar macrophages (AM) and increased the viability of AM. However, even after treatment with GO, Kp was still able to cause infection to a certain extent compared with untreated mice. This suggests that the antimicrobial activity of GBNs differs between the bacterial and animal levels. This phenomenon may be due to the complex *in vivo* environment, where factors such as the immune system, pharmacokinetics, and physiological barriers affect the efficacy of GBNs.

5.2. As drug carriers

It is an effective strategy to improve the antibacterial effect by using delivery carriers to accurately deliver therapeutic drugs to the infected site. Nanoparticle-based drug delivery systems have some unique superiorities, such as prolong drug retention time in blood, reducing nonspecific distribution and targeted delivering the therapeutics to the site of infections.[60] Graphene and its derivatives are able to conjugate with other aromatic materials on the surface through the π–π stacking, and the large surface area of graphene makes multi-drug delivery possible. In addition, GO and rGO have a large amount of carboxyl groups and hydroxyl groups that are enough to form various chemical interactions. Therefore, GBNs can be designed as drug delivery carriers *via* combining with other substances. Nowadays, functionalized graphene derivatives, such as GO, rGO, carbon nanotubes, and graphite have been successfully applied to develop stimuli-responsive nanocarriers that load various molecules such as genes, small drug molecules, nucleic acid, antibodies and proteins. For example, S. Sanaei-Rad *et al.*[65] constructs a nanoparticle ZIF-8/GO/$MgFe_2O_4$ for delivering tetracycline towards bacteria, which improve the antibacterial activities against both Gram-positive and Gram-negative bacteria. Y. Ning *et al.*[66] loaded a penicillin-binding protein 2a (PBP2a)-targeted aptamer and berberine onto the surface of GO which significantly inhibiting MRSA biofilm formation. GO-immobilized titanium dioxide (TiO_2) was developed to efficiently carry and release doxycycline hyclate (Dox) *via* non-covalent interactions, including electrostatic interaction, π–π stacking, hydrophobic interaction, and hydrogen bonds. The amount of loaded drug was able to reach a maximum of 36 μg

Table 2 Therapeutic molecules loaded onto graphene-based materials[a]

Materials	Delivered molecule	Functionalization	Target	Ref.
Ly-PDA@GO/CS-Arg	Lysozyme	Dopmine	*E. coli* and *S. aureus*	68
GO-AMOX-BROM hydrogel	AMOX	—	*E. faecalis*	69
Dox/GOTA/TiO_2	Dox	—	*E. coli* and *S. aureus*	67
GO-PEG-CEF	Cephalexin	PEG	*S. aureus* and *B. cereus*	70
NO-doped F-PEG@GO	NO	F-PEG	*E. coli* and *S. aureus*	71
pGO-TCH	TCH	PEI	*S. aureus* and *E. coli*	72
GO-PEG	Oxacillin, penicillin	PEG	MRSA	73
ZIF-8/GO/$MgFe_2O_4$	Tetracycline	$MgFe_2O_4$	*S. aureus* and *E. coli*	74 65
GO-PEG	Nigella sativa seed extract	PEG	*S. aureus* and *E. coli*	74
CMC/MOF-5/GO	Tetracycline	—	*E. coli*	75

[a] F-PEG: fluorinated poly ethylene glycol; PEI: polyethyleneimine; AMOX: amoxicillin; TCH: tetracycline hydrochloride; BROM: bromelain.

cm^{-2}.[67] The obtained results indicated that GBNs are effective carriers for antimicrobial drug delivery. Table 2 summarizes some antimicrobial agents that have been loaded onto graphene-based materials.

5.3. Photodynamic therapy (PDT)

Photodynamic therapy (PDT), as a therapeutic technique with low invasiveness and mild adverse effects that take effect depending on photo-triggered generation of cytotoxic ROS, has been proved to be an efficacious strategy to fight against microbial pathogens.[76–79] ROS-induced oxidative stress can destroy the surrounding essential biomolecules, such as lipids, proteins, and nucleic acids, and finally leads to bacterial death.[80,81] Nowadays, PDT has been utilized in clinical treatment of refractory local infectious diseases, and retards the development of MDR caused by switching antibiotics or tapering their administration dose.[82] GODs have been used to improve the biocompatibility of organic photosensitizers for bioimaging and even entirely replace organic photosensitizers in PDT owing to their tunable optical and electronic properties.[83,84] GQD killed MRSA and *Escherichia coli* by generating reactive oxygen species when photoexcited (470 nm, 1 W). Neither GQD nor light exposure alone were able to cause oxidative stress and reduce the viability of bacteria.[85] However, the low tissue penetrance of blue light and low absorbance of GQDs at high wavelengths limit the application of photodynamic therapy based on GQDs in bacterial infections.

5.4. Photothermal therapy (PTT)

Photothermal therapy (PTT) has emerged as a promising approach due to its controllable and tiny invasive mechanism high efficiency, spatiotemporal controllability, and deep tissue penetration.[86–88] Unlike traditional antibiotics, PTT leverages near-infrared (NIR) radiation to induce localized hyperthermia, destroying bacterial membranes and effectively killing pathogens, while avoiding the emergence of bacterial drug resistance. This characteristic makes PTT a compelling alternative to conventional antibacterial therapies, especially when dealing with drug-resistant infections.[89] Specifically, PTT can trigger changes in cell membrane permeability and fluctuations in intracellular enzyme activity when the temperature is in the range of 41 °C to 47 °C, while it can cause cell membrane damage and protein denaturation when the temperature exceeds 50 °C. P. Li. *et al.*[20] synthesized highly graphitic-N-doped graphene quantum dots (N-GQDs) with efficient NIR-II photothermal conversion properties were synthesized for the first time for PTT. The obtained N-GQDs exhibited strong NIR absorption ranging from 700 to 1200 nm, achieving high photothermal conversion efficiency of 77.8% and 50.4% at 808 and 1064 nm, respectively. Outstanding antibacterial and antibiofilm activities against MDR bacteria were achieved by the N-GQDs in the presence of an 808 or 1064 nm. Qu[57] designed a novel near-infrared light responsive platform for targeted imaging and photothermal killing of drug-resistant bacteria based on multifunctional rGO *via* attaching vancomycin (Van) and a europium (Eu^{3+}) complex. Van functioned as a target agent to capture bacteria by contacting with terminal D-Ala–D-Ala moieties of peptide units located on the bacterial cell walls. Eu^{3+} complex could emit strong red luminescence upon excitation so as to act as an imaging agent for bacteria tracking. Van-modified rGO (Van-rGO) could strongly absorb NIR radiation and transfer this energy into the surrounding environment as heat, thus resulting in the death of bacteria. All of the Gram-negative bacteria (10^8 CFU mL^{-1}) and less than 3% of Gram-positive bacteria that survived were killed at a Van-rGO concentration of 10 mg mL^{-1} under NIR light irradiation for 3 min (808 nm, 1.5 W cm^2). However, some drawbacks hinder the practical application of PTT. For example, photothermal nano-agents themselves cannot selectively target pathogenic bacteria or biofilms, which may result in a limited therapeutic efficacy and damage to the surrounding healthy tissues.[90,108] Besides, current operating temperature of PTT is too high (55–60 °C), which may burn the normal skin and other tissues.[91] Moreover, the curative effect of monotherapy is not equal to expected in treating bacterial infections.[89]

6. Combining with other therapeutic strategies

In order to improve the antibacterial properties of nanomaterials, researchers have developed manifold combinatorial

therapies to effectively combat MDR, such as combining other antimicrobial materials, traditional antibiotics, peptides and so on. Nanocomposites transcend the limitations of single-component materials by harnessing the synergistic effects and composite functionalities of multiple components. They exhibit remarkable advantages in combating drug-resistant bacteria, primarily manifested in the diversity of antimicrobial mechanisms, high efficacy, biocompatibility, targeting capabilities, and multifunctional synergistic effects.

6.1. Combining with other nanometer to fight MDR bacteria

Due to the easily functionalized structure of GBNs, their antibacterial activity can be enhanced *via* forming nanocomposites with other nanomaterials or bioactive agents, such as metal or metal oxide-based nanomaterials.[92] It is reported that metal nanoparticles (NPs) can interact with the GO sheets through electrostatic binding, physisorption, and charge-transfer interactions. Compared with pure rGO nanosheets and AuNS, the rGO/gold nanopillar (rGO/AuNS) nanocomposites not only improved the photothermal conversion but also showed good intrinsic antibacterial activity and significantly enhanced the interaction with bacteria.[92] Silver (Ag) is a powerful antimicrobial material which can prevent serious infections by inactivating enzymes related to bacterial metabolism, disrupting bacterial membranes, and inhibiting DNA replication.[93] Ag nanoparticles have a wide antibacterial spectrum and have high potential to solve multi drug resistance bacterial like *Acinetobacter baumannii*, Kp, and PA.[94,95] However, spontaneous aggregation of Ag nanoparticles makes the antibacterial ability decrease.[23] GO surface modification and functionalization of NPs improve the stability and dispersibility and thus solve the drawbacks of Ag NPs.[96,97] In turn, Ag enhances the antibacterial ability of GO nanomaterials. X. Guo *et al.*[98] synthesized a binary graphene oxide and copper iron sulfide nanocomposite (GO/$CuFeS_x$ NC) to fight against the MDR bacteria and biofilm. Compared with CuS NPs, iron decoration contributes to the favorable distribution of bimetallic $CuFeS_x$ NPs on the GO surface, which synergistically enhances peroxidase-like activity and intrinsic strong near-infrared (NIR) light-responsive photothermal activity in acidic media. The ultrathin and sharp structure of the two-dimensional GO nanosheets enables GO/$CuFeS_x$ NCs to strongly interact with bacteria and biofilms, thereby facilitating catalytic and photothermal attacks on bacterial surfaces. J. Liu *et al.*[28] synthesized a multifunctional two-dimensional nanosheet (SGQDs-CORM@HA, SCH) which conjunct CO-releasing molecules (CORM-401) and hyaluronic acid (HA) onto single-layered graphene quantum dots (SGQDs) for selectively eradicating MRSA *via* cascade-activated photodynamic/CO gas therapy. Compared with PBS control, vancomycin and "SGQDs + light" showed the fastest wound healing, lowest neutrophil scattering in skin lesion and bacterial CFU number. In summary, composite nanomaterials are able to complement each other and combine multiple therapeutic strategies (PDT, PTT, gas therapy, *etc.*) to enhance antimicrobial activity.

6.2. Combining with antimicrobial peptides (AMPs)

As is known, AMPs, small peptide sequences that feature a positive charge and hydrophobic residues, can target and kill bacterial cells through various mechanisms, such as disrupting the cell membrane by forming pores through depolarization.[99] Compared to traditional antibiotics, AMPs display several distinct advantages, including a broad range of antimicrobial activities, a quick mode of action, a relatively high degree of target specificity towards microbial membranes, and, most significantly, a low incidence of resistant bacterial strain emergence.[100] However, AMPs have limited clinical applications, mainly due to their high toxicity to mammalian cells.[101] Recent studies have shown that the bactericidal efficacy of AMPs can be improved by decorating them on the surface of nanoparticles or by self-assembling AMP-based derivatives into nanostructures.[10,102–104] Furthermore, immobilizing AMPs on nanomaterials could enhance the long-term stability and activity of AMPs.[103] Ma *et al.* decorated melittin peptide on the edges of graphene/GO nanosheets and achieved an up to 20-fold enhancement in the antibacterial activity.[104] Tryptophan (Trp) and arginine (Arg) are known to be necessary for antimicrobial peptides to exert their antimicrobial effects. The Arg residues confer cationic charge and hydrogen bonding properties to AMPs and are able to interact with the abundant anionic component of the bacterial membrane. Meanwhile, Trp residues show a distinct preference for the interfacial region of lipid bilayers.[101,103,105] N. A. Samak *et al.*[103] synthesized a cyclic dodecapeptide peptide (Cdp) which added three additional mutants to enrich the Arg and Trp residues in different ratios. After, the dodecapeptides were immobilized on a rGO nanocomposite anchored with a hierarchical β-MnO_2 (rGO/β-MnO_2) hybrid. The immobilized Cdp-4/rGO/β-MnO_2 AMP showed excellent properties against the multidrug-resistant PA ATCC 15692 planktonic cells with an MIC value of 0.97 μg mL^{-1}. In addition, combining peptides with nanoparticles is expected to achieve targeted identification of bacteria considering that AMPs can specifically interact with bacterial membranes. S. K. *et al.* functionalized rGO/Ag with poly-L-lysine (PLL), a natural AMP, and achieved target specificity against the *S. aureus* biofilm.[97] To sum up, bioconjugation of peptides to nanoparticles not only specifically identify bacteria, improve antibacterial efficiency, but also protect peptides from being cleaved by intracellular enzymes.[102,106]

6.3. Combining with photosensitizer for bacterial tracking

Rapid, accurate and precise diagnostic methods possess great importance to focus on appropriate antibacterial treatments. Development of nanotechnology offers new possibilities for bacterial tracing. Although GNBs themselves cannot act as bacterial tracers, they can illuminate bacteria by combining with other light-emitting materials. The unique properties of rare earth (RE) complexes have been applied in the fields of LED devices, optical coding, luminescence imaging/detection and time-resolved luminescence detection due to their unique properties such as ligand-sensitized energy transfer, fingerprint-like emission and long-lived emission. *In vitro* and *in vivo* imaging

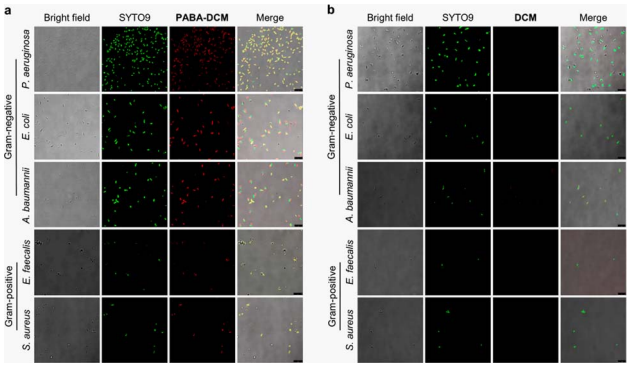

Fig. 6 Representative fluorescence images of bacterial *in vitro*. Representative fluorescence images of different Gram-negative bacterial strains incubated with (a) PABA-DCM (10 μM) and (b) DCM (10 μM) for 2 h and analyzed by a confocal-scanning laser microscope. Reproduced with permission.[108] Copyright 2022, American Chemical Society.

using RE luminescent materials can easily eliminate the interference of autofluorescence and any background fluorescence of the organism. X. Yang[57] functionalized Van-rGO with a europium (Eu^{3+}) complex through EDC/NHS chemistry for targeted imaging. Both of DR-*E. coli* and DR-*S. aureus* were illuminated after10 min incubation with Eu-Van-rGO and red photoluminescence were observed by the naked eye upon UV excitation. NGO-BSA-AIE NPs formulated by NGO, BSA and aggregation induced emission fluorogen (AIEgen) *via* hydrophobic interactions were developed as an antibacterial nanomaterial for dual-mode phototherapy. AIEgen acted not only as a photosensitizer for killing bacteria, but also as a fluorescent probe for tracking the distribution of bacteria.[34] *C. glomerata* is one of the most widespread filamentous green freshwater macroalgae found in eutrophic freshwaters and is capable of photosynthesis.[107] Zhong *et al.*[108] constructed a fluorescent imaging probe, PABA-DCM, *via* conjugating *p*-aminobenzoic acid (PABA) with a long-wavelength fluorophore, dicyanomethylene 4H-pyran (DCM). Then, a hydrogel-based dressing (PABA-DCM@GO) was prepared using gelatin, GO and PABA-DCM for targeted fluorescence visualization of bacterial infections on mouse wounds. The results showed that intense PABA-DCM fluorescence was detected in all bacterial species used for imaging (Fig. 6a), while almost no DCM fluorescence was detected (Fig. 6b). As seen in Fig. 7a, five different live bacteria including PA, *E. coli*, *A. baumannii*, *E. faecalis*, and *S. aureus* were injected in the left wound and dead bacteria with heat pretreatment were injected in the right wound to establish infected and non-infected models. After 2 hours of applying PABA-DCM@GO hydrogel dressing, the fluorescence intensity of the infected tissue on the left was significantly stronger than that of the non-infected tissue on the right (Fig. 7b and c). Therefore, modification of GBNs with fluorescent agent possesses significant potential for bacterial distribution imaging.

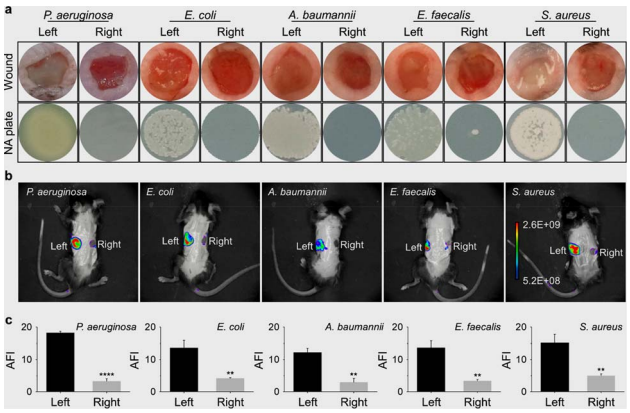

Fig. 7 (a) Photos of wounds on both sides of implant-related mice treated with viable bacteria (10^6 CFU mL^{-1}) (left wound) and heat-killed bacteria (10^7 CFU mL^{-1}) (right wound). (b) Fluorescence imaging of implant-related wound infection mice models treated with PABA-DCM@GO (PABA-DCM/GO = 10 μM/100 μg mL^{-1}). (c) Fluorescence quantification of the right and left wound of the mice treated with PABA-DCM@GO. Reproduced with permission.[108] Copyright 2022, American Chemical Society.

7. Summary and outlook

The management of multidrug-resistant (MDR) bacterial infections has long posed a significant challenge in clinical settings. The mechanisms underlying bacterial resistance are intricate and multifaceted, encompassing the production of enzymes that inactivate drugs (such as β-lactamases), modifications to drug targets (for instance, alterations in penicillin-binding proteins), diminished cell membrane permeability, and the formation of protective biofilms.[109,110] Biofilms, in particular, act as a physical barrier that obstructs the entry of antibiotics and facilitates bacterial survival in adverse conditions. Consequently, there is an urgent need for innovative, non-traditional therapeutic approaches to combat drug-resistant bacteria.

The tunable surface function and antimicrobial properties of graphene provide a versatile platform for designing novel antimicrobial agents to combat multidrug resistant bacterial infections. In this review, we attempt to summarize the recent achievements and progress of GBNs for applications in the antibacterial field. In this tutorial, we have discussed multiple strategies that utilize GBNs as (i) self-therapeutic agents. (ii) Carriers for antimicrobial cargo. (iii) Combined with a variety of materials to detect bacterial infections and enhanced antibacterial effectiveness. As we know, the bacterial resistance to antibiotics is largely due to the abuse or repeated long-term use of antibiotics. Therefore, the antibacterial effects of GBNs are of great importance for the effective antibacterial therapy since their mechanisms are antibiotics-independent. GBNs can kill pathogens through multiple mechanisms, including cutting effect, oxidative stress and cell entrapment. However, there were several challenges hinder their clinical usage, such as biosafety issues, limited applicable organs and easy aggregation in physiological environment. To solve these problems, experts have attempted to modify GBNs using various substances, including small molecules, nanoparticles and polymers. By forming composites with these substances, GBNs can improve biocompatibility and targeting effects, leading to improved

biosafety and delivery efficiency. For instance, incorporating other nanomaterials with GBNs can significantly enhance their dispersion and stability within physiological environments. This combination not only mitigates the tendency of GBNs to aggregate but may also elicit synergistic effects, thereby augmenting their overall antimicrobial activity. Moreover, different nanomaterials possess distinct antimicrobial mechanisms, and their synergistic application offers multiple routes of bacterial eradication, making it challenging for bacteria to develop resistance. AMPs, despite their potent antimicrobial properties, are prone to enzymatic degradation *in vivo*, which can rapidly inactivate them. By immobilizing AMPs onto GBNs, these peptides are shielded from enzymatic attack, thus extending their functional lifespan and enhancing their therapeutic efficacy. Photosensitizers, on the other hand, generate ROS upon irradiation with specific wavelengths of light, exerting antibacterial effects while also emitting fluorescence that can be harnessed for bacterial tracking. Integrating GBNs with photosensitizers enables the concurrent realization of bacterial localization and treatment. Furthermore, GBNs' excellent light-absorbing capabilities allow them to convert absorbed light energy into heat, thereby amplifying the ROS production by photosensitizers through a synergistic thermal effect. This combined approach not only enhances the antimicrobial efficacy but also ensures precise targeting of bacterial infections.

Another important difficulty is that the mononuclear phagocytic system can eliminate nanoparticles from the blood stream which resulting in reduced antimicrobial efficacy. Therefore, the surface of the nanoparticles needs to be cleverly designed to escape recognition by the immune system. Although several studies have attempted to construct biomimetic nanoparticles, the results have been unsatisfactory. A great deal of work remains to be done to explore the indications of graphene in MDR bacterial infections and to further provide rich theoretical support from laboratory to clinical applications.

Data availability

No primary research results, software or code have been included and no new data were generated or analysed as part of this review.

Author contributions

X. L. and S. C. conceived and designed the overall structure of the review; J. C., Y. W. and X. H. retrieved and screened the literature, interpreted it in detail, and summarized the key points; J. H. wrote the paper and led the project; H. Z. assisted in editing and proofreading the full text. All authors have read and agreed to the published version of the manuscript.

Conflicts of interest

The authors have no conflicts of interest to declare.

Acknowledgements

This work was supported by the Clinical Medicine Translation Special Program of the Key Research and Development Plan in Anhui Province (202204295107020033).

References

1 GBD 2021 Antimicrobial Resistance Collaborators, *Lancet*, 2024, **404**, 1199–1226.
2 X. Liu, J. Li, Z. Zhang, Y. He, M. Wang, Y. Zhao, S. Lin, T. Liu, Y. Liao, N. Zhang, K. Yuan, Y. Ling, Z. Liu, X. Chen, Z. Chen, R. Chen, X. Wang and B. Gu, *Nucleic Acids Res.*, 2024, **52**, 2886–2903.
3 Y. Yang, Y. Yan, C. J. Schofield, A. McNally, Z. Zong and G. Li, *Trends Microbiol.*, 2023, **31**, 735–748.
4 P. Brindangnanam, A. R. Sawant, K. Ashokkumar, K. Sriraghavan, S. P. K. Prashanth and M. S. Coumar, *Microb. Pathog.*, 2025, **203**, 107513.
5 M. Ding, W. Zhao, L. Song and S. Luan, *Rare Met.*, 2022, **41**, 482–498.
6 M. Miethke, M. Pieroni, T. Weber, M. Bronstrup, P. Hammann, L. Halby, P. B. Arimondo, P. Glaser, B. Aigle, H. B. Bode, R. Moreira, Y. Li, A. Luzhetskyy, M. H. Medema, J. Pernodet, M. Stadler, J. R. Tormo, O. Genilloud, A. W. Truman, K. J. Weissman, E. Takano, S. Sabatini, E. Stegmann, H. Brotz-Oesterhelt, W. Wohlleben, M. Seemann, M. Empting, A. K. H. Hirsch, B. Loretz, C. Lehr, A. Titz, J. Herrmann, T. Jaeger, S. Alt, T. Hesterkamp, M. Winterhalter, A. Schiefer, K. Pfarr, A. Hoerauf, H. Graz, M. Graz, M. Lindvall, S. Ramurthy, A. Karlen, M. van Dongen, H. Petkovic, A. Keller, F. Peyrane, S. Donadio, L. Fraisse, L. J. V. Piddock, I. H. Gilbert, H. E. Moser and R. Muller, *Nat. Rev. Chem.*, 2021, **5**, 726–749.
7 X. Song, P. Liu, X. Liu, Y. Wang, H. Wei, J. Zhang, L. Yu, X. Yan and Z. He, *Mater. Sci. Eng., C*, 2021, **128**, 112318.
8 M. Alavi and M. Rai, *Expert Rev. Anti-Infect. Ther.*, 2019, **17**, 419–428.
9 A. Baker, A. Syed, A. A. Alyousef, M. Arshad, A. Alqasim, M. Khalid and M. S. Khan, *Microb. Pathog.*, 2020, **148**, 104467.
10 S. J. Lam, N. M. O'Brien-Simpson, N. Pantarat, A. Sulistio, E. H. H. Wong, Y. Chen, J. C. Lenzo, J. A. Holden, A. Blencowe, E. C. Reynolds and G. G. Qiao, *Nat. Microbiol.*, 2016, **1**, 16162.
11 B. Bagheri, S. S. Surwase, S. S. Lee, H. Park, Z. Faraji Rad, N. L. Trevaskis and Y. Kim, *J. Mater. Chem. B*, 2022, **10**, 9944–9967.
12 M. Xia, Y. Xie, C. Yu, G. Chen, Y. Li, T. Zhang and Q. Peng, *J. Controlled Release*, 2019, **307**, 16–31.
13 N. Chatterjee, J. Yang and J. Choi, *Mutat. Res., Genet. Toxicol. Environ. Mutagen.*, 2016, **798–799**, 1–10.
14 V. Ramalingam, S. Raja, S. Sundaramahalingam and R. Rajaram, *Bioorg. Chem.*, 2019, **83**, 326–335.

15 M. Yousefi, M. Dadashpour, M. Hejazi, M. Hasanzadeh, B. Behnam, M. de la Guardia, N. Shadjou and A. Mokhtarzadeh, *Mater. Sci. Eng., C*, 2017, **74**, 568–581.
16 Y. Gao, Y. Dong, Y. Cao, W. Huang, C. Yu, S. Sui, A. Mo and Q. Peng, *J. Biomed. Nanotechnol.*, 2021, **17**, 1627–1634.
17 Y. Chen, W. Wu, Z. Xu, C. Jiang, S. Han, J. Ruan and Y. Wang, *R. Soc. Open Sci.*, 2020, **7**, 192019.
18 S. Ullah, A. Ahmad, F. Subhan, A. Jan, M. Raza, A. U. Khan, A. Rahman, U. A. Khan, M. Tariq and Q. Yuan, *J. Photochem. Photobiol., B*, 2018, **183**, 342–348.
19 D. Z. Zmejkoski, Z. M. Markovic, D. D. Mitic, N. M. Zdravkovic, N. O. Kozyrovska, N. Bugarova and B. M. Todorovic Markovic, *J. Biomed. Mater. Res., Part B*, 2022, **110**, 1796–1805.
20 B. Geng, Y. Li, J. Hu, Y. Chen, J. Huang, L. Shen, D. Pan and P. Li, *J. Mater. Chem. B*, 2022, **10**, 3357–3365.
21 M. A. Zarouki, L. Tamegart, L. Hejji, Y. A. El Hadj Ali, A. E. Ayadi, L. P. Villarejo, Z. Mennane, B. Souhail and A. Azzouz, *Int. J. Pharm.*, 2024, **649**, 123658.
22 F. Z. E. D. Naseer, *J. Environ. Chem. Eng.*, 2020, **5**, 104424.
23 P. Lozovskis, V. Jankauskaite, A. Guobiene, V. Kareiviene and A. Vitkauskiene, *Int. J. Nanomed.*, 2020, **15**, 5147–5163.
24 S. Tan, X. Wu, Y. Xing, S. Lilak, M. Wu and J. X. Zhao, *Colloids Surf., B*, 2020, **185**, 110616.
25 B. Zhao, H. Wang, W. Dong, S. Cheng, H. Li, J. Tan, J. Zhou, W. He, L. Li, J. Zhang, G. Luo and W. Qian, *J. Nanobiotechnol.*, 2020, **18**, 59.
26 H. Hu, X. Kang, Z. Shan, X. Yang, W. Bing, L. Wu, H. Ge and H. Ji, *Nanoscale*, 2022, **14**, 2676–2685.
27 P. Pandey, R. Sahoo, K. Singh, S. Pati, J. Mathew, A. C. Pandey, R. Kant, I. Han, E. Choi, G. R. Dwivedi and D. K. Yadav, *Nanomaterials*, 2021, **12**, 117.
28 J. Liu, R. S. Li, M. He, Z. Xu, L. Q. Xu, Y. Kang and P. Xue, *Biomaterials*, 2021, **277**, 121084.
29 M. Oves, M. A. Rauf, M. O. Ansari, A. A. P. Khan, H. A. Qari, M. F. Alajmi, S. Sau and A. K. Iyer, *Nanomaterials*, 2020, **10**, 1004.
30 C. Xing, J. Chang, M. Ma, P. Ma, L. Sun and M. Li, *J. Colloid Interface Sci.*, 2022, **612**, 664–678.
31 Y. Feng, Q. Chen, Q. Yin, G. Pan, Z. Tu and L. Liu, *ACS Appl. Bio Mater.*, 2019, **2**, 747–756.
32 W. Pan, C. Huang, T. Lin, H. Hu, W. Lin, M. Li and H. Sung, *Nanomedicine*, 2016, **12**, 431–438.
33 X. Yang, Z. Li, E. Ju, J. Ren and X. Qu, *Chem.–Eur. J.*, 2014, **20**, 394–398.
34 Y. Zhang, H. Fu, D. Liu, J. An and H. Gao, *J. Nanobiotechnol.*, 2019, **17**, 104.
35 S. Shamsi, A. A. H. Abdul Ghafor, N. H. Norjoshukrudin, I. M. J. Ng, S. N. S. Abdullah, S. N. E. Sarchio, F. Md Yasin, S. Abd Gani and M. N. Mohd Desa, *Int. J. Nanomed.*, 2022, **17**, 5781–5807.
36 M. K. Rabchinskii, S. A. Ryzhkov, D. A. Kirilenko, N. V. Ulin, M. V. Baidakova, V. V. Shnitov, S. I. Pavlov, R. G. Chumakov, D. Y. Stolyarova, N. A. Besedina, A. V. Shvidchenko, D. V. Potorochin, F. Roth, D. A. Smirnov, M. V. Gudkov, M. Brzhezinskaya, O. I. Lebedev, V. P. Melnikov and P. N. Brunkov, *Sci. Rep.*, 2020, **10**, 6902.
37 J. Liu, S. Bao and X. Wang, *Micromachines*, 2022, **13**, 184.
38 N. Krasteva, M. Keremidarska-Markova, K. Hristova-Panusheva, T. Andreeva, G. Speranza, D. Wang, M. Draganova-Filipova, G. Miloshev and M. Georgieva, *Oxid. Med. Cell. Longevity*, 2019, **2019**, 3738980.
39 V. T. Le, Y. Vasseghian, E. Dragoi, M. Moradi and A. Mousavi Khaneghah, *Food Chem. Toxicol.*, 2021, **148**, 111931.
40 H. Huang, K. K. H. De Silva, G. R. A. Kumara and M. Yoshimura, *Sci. Rep.*, 2018, **8**, 6849.
41 O. C. Compton and S. T. Nguyen, *Small*, 2010, **6**, 711–723.
42 H. Huang, K. K. H. De Silva, G. R. A. Kumara and M. Yoshimura, *Sci. Rep.*, 2018, **8**, 6849.
43 B. S. Dash, Y. Lu, P. Pejrprim, Y. Lan and J. Chen, *Biomater. Adv.*, 2022, **136**, 212764.
44 B. S. Dash, G. Jose, Y. Lu and J. Chen, *Int. J. Mol. Sci.*, 2021, **22**, 6658.
45 R. Liu, X. Wang, J. Ye, X. Xue, F. Zhang, H. Zhang, X. Hou, X. Liu and Y. Zhang, *Nanotechnology*, 2018, **29**, 105704.
46 X. Chen, K. Fan, Y. Liu, Y. Li, X. Liu, W. Feng and X. Wang, *Adv. Mater.*, 2022, **34**, e2101665.
47 W. Feng, P. Long, Y. Feng and Y. Li, *Adv. Sci.*, 2016, **3**, 1500413.
48 H. Geng, T. Wang, H. Cao, H. Zhu, Z. Di and X. Liu, *Colloids Surf., B*, 2019, **173**, 681–688.
49 V. Kansara, S. Tiwari and M. Patel, *Colloids Surf., B*, 2022, **217**, 112605.
50 A. Anand, B. Unnikrishnan, S. Wei, C. P. Chou, L. Zhang and C. Huang, *Nanoscale Horiz.*, 2019, **4**, 117–137.
51 L. Hui, J. Huang, G. Chen, Y. Zhu and L. Yang, *ACS Appl. Mater. Interfaces*, 2016, **8**, 20–25.
52 K. Kholikov, S. Ilhom, M. Sajjad, M. E. Smith, J. D. Monroe, O. San and A. O. Er, *Photodiagn. Photodyn. Ther.*, 2018, **24**, 7–14.
53 W. Wu, Y. Qin, Y. Fang, Y. Zhang, S. Shao, F. Meng and M. Zhang, *J. Hazard. Mater.*, 2023, **441**, 129954.
54 W. Hu, C. Peng, W. Luo, M. Lv, X. Li, D. Li, Q. Huang and C. Fan, *ACS Nano*, 2010, **4**, 4317–4323.
55 F. Perreault, A. F. de Faria, S. Nejati and M. Elimelech, *ACS Nano*, 2015, **9**, 7226–7236.
56 V. Palmieri, F. Bugli, M. C. Lauriola, M. Cacaci, R. Torelli, G. Ciasca, C. Conti, M. Sanguinetti, M. Papi and M. De Spirito, *ACS Biomater. Sci. Eng.*, 2017, **3**, 619–627.
57 X. Yang, Z. Li, E. Ju, J. Ren and X. Qu, *Chem.–Eur. J.*, 2014, **20**, 394–398.
58 J. W. D. G. Qiu, *Adv. Mater. Interfaces*, 2017, **15**, 1700228.
59 M. L. Q. L. Wang, *Appl. Surf. Sci.*, 2018, **448**, 351–361.
60 A. Gupta, S. Mumtaz, C. H. Li, I. Hussain and V. M. Rotello, *Chem. Soc. Rev.*, 2019, **48**, 415–427.
61 M. Bahrami, P. Serati Shirazi, F. Moradi, N. Hadi, N. Sabbaghi and S. Eslaminezhad, *Microb. Pathog.*, 2024, **196**, 107002.
62 C. Wang, S. M. S. Shahriar, Y. Su and J. Xie, *Nanomedicine*, 2025, **20**, 501–518.
63 O. Akhavan and E. Ghaderi, *ACS Nano*, 2010, **4**, 5731–5736.
64 X. Wu, S. Tan, Y. Xing, Q. Pu, M. Wu and J. X. Zhao, *Colloids Surf., B*, 2017, **157**, 1–9.

65 S. Sanaei-Rad, M. A. Ghasemzadeh and S. M. H. Razavian, *Sci. Rep.*, 2021, **11**, 18734.
66 Y. Ning, X. Wang, P. Chen, S. Liu, J. Hu, R. Xiao, L. Li and F. Lu, *Drug Delivery*, 2022, **29**, 1675–1683.
67 D. L. Tran, P. Le Thi, T. T. Hoang Thi and K. D. Park, *Colloids Surf., B*, 2019, **181**, 576–584.
68 C. Fu, Z. Qi, C. Zhao, W. Kong, H. Li, W. Guo and X. Yang, *J. Biol. Eng.*, 2021, **15**, 17.
69 A. Trusek and E. Kijak, *Materials*, 2021, **14**, 3182.
70 N. P. Katuwavila, Y. Amarasekara, V. Jayaweera, C. Rajaphaksha, C. Gunasekara, I. C. Perera, G. A. J. Amaratunga and L. Weerasinghe, *J. Pharm. Sci.*, 2020, **109**, 1130–1135.
71 Y. A. Workie, Sabrina, T. Imae and M. P. Krafft, *ACS Biomater. Sci. Eng.*, 2019, **5**, 2926–2934.
72 L. Jiang, C. Su, S. Ye, J. Wu, Z. Zhu, Y. Wen, R. Zhang and W. Shao, *Nanotechnology*, 2018, **29**, 505102.
73 M. Mohammadi Tabar, M. Khaleghi, E. Bidram, A. Zarepour and A. Zarrabi, *Pharmaceutics*, 2022, **14**, 2049.
74 M. A. Jihad, F. T. M. Noori, M. S. Jabir, S. Albukhaty, F. A. AlMalki and A. A. Alyamani, *Molecules*, 2021, **26**, 3067.
75 Z. Karimzadeh, S. Javanbakht and H. Namazi, *BioImpacts*, 2019, **9**, 5–13.
76 S. Clement and J. Winum, *Expert Opin. Ther. Pat.*, 2024, **34**, 401–414.
77 Q. Jia, Q. Song, P. Li and W. Huang, *Adv. Healthcare Mater.*, 2019, **8**, e1900608.
78 X. Hu, Y. Huang, Y. Wang, X. Wang and M. R. Hamblin, *Front. Microbiol.*, 2018, **9**, 1299.
79 G. Wei, G. Yang, Y. Wang, H. Jiang, Y. Fu, G. Yue and R. Ju, *Theranostics*, 2020, **10**, 12241–12262.
80 A. Bekmukhametova, H. Ruprai, J. M. Hook, D. Mawad, J. Houang and A. Lauto, *Nanoscale*, 2020, **12**, 21034–21059.
81 L. M. de Freitas, E. N. Lorenzon, N. A. Santos-Filho, L. H. D. P. Zago, M. P. Uliana, K. T. de Oliveira, E. M. Cilli and C. R. Fontana, *Sci. Rep.*, 2018, **8**, 4212.
82 W. Ma, X. Chen, L. Fu, J. Zhu, M. Fan, J. Chen, C. Yang, G. Yang, L. Wu, G. Mao, X. Yang, X. Mou, Z. Gu and X. Cai, *ACS Appl. Mater. Interfaces*, 2020, **12**, 22479–22491.
83 Z. Li, D. Wang, M. Xu, J. Wang, X. Hu, S. Anwar, A. C. Tedesco, P. C. Morais and H. Bi, *J. Mater. Chem. B*, 2020, **8**, 2598–2606.
84 C. Shih, W. Huang, I. Chiang, W. Su and H. Teng, *Nanoscale*, 2021, **13**, 8431–8441.
85 B. Z. Ristic, M. M. Milenkovic, I. R. Dakic, B. M. Todorovic-Markovic, M. S. Milosavljevic, M. D. Budimir, V. G. Paunovic, M. D. Dramicanin, Z. M. Markovic and V. S. Trajkovic, *Biomaterials*, 2014, **35**, 4428–4435.
86 Y. Yu, H. Zhao, J. Liu, C. Li, P. Liu, P. Cheng, Y. Liu, W. Guo, F. Guan and M. Yao, *Int. J. Biol. Macromol.*, 2025, **300**, 140325.
87 G. Gao, Y. Jiang, H. Jia and F. Wu, *Biomaterials*, 2019, **188**, 83–95.
88 C. Zhang, S. Fan, J. Zhang, G. Yang, C. Cai, S. Chen, Y. Fang and W. Wan, *Bioact. Mater.*, 2025, **50**, 232–245.
89 C. Mao, Y. Xiang, X. Liu, Y. Zheng, K. W. K. Yeung, Z. Cui, X. Yang, Z. Li, Y. Liang, S. Zhu and S. Wu, *ACS Appl. Mater. Interfaces*, 2019, **11**, 17902–17914.
90 W. Qian, C. Yan, D. He, X. Yu, L. Yuan, M. Liu, G. Luo and J. Deng, *Acta Biomater.*, 2018, **69**, 256–264.
91 M. Liu, D. He, T. Yang, W. Liu, L. Mao, Y. Zhu, J. Wu, G. Luo and J. Deng, *J. Nanobiotechnol.*, 2018, **16**, 23.
92 H. Wang, N. Mu, Y. He, X. Zhang, J. Lei, C. Yang, L. Ma and Y. Gao, *Theranostics*, 2023, **13**, 1669–1683.
93 W. Xu, X. Qing, S. Liu, Z. Chen and Y. Zhang, *J. Mater. Chem. B*, 2022, **10**, 1343–1358.
94 N. Nino-Martinez, G. A. Martinez-Castanon, A. Aragon-Pina, F. Martinez-Gutierrez, J. R. Martinez-Mendoza and F. Ruiz, *Nanotechnology*, 2008, **19**, 65711.
95 D. Pissuwan, C. H. Cortie, S. M. Valenzuela and M. B. Cortie, *Trends Biotechnol.*, 2010, **28**, 207–213.
96 T. Xia, X. Guo, Y. Lin, B. Xin, S. Li, N. Yan and L. Zhu, *Environ. Pollut.*, 2019, **251**, 921–929.
97 T. Parandhaman, P. Choudhary, B. Ramalingam, M. Schmidt, S. Janardhanam and S. K. Das, *ACS Biomater. Sci. Eng.*, 2021, **7**, 5899–5917.
98 X. Guo, X. Zhang, M. Yu, Z. Cheng, Y. Feng and B. Chen, *J. Colloid Interface Sci.*, 2024, **661**, 802–814.
99 A. K. Sandhu, Y. Yang and W. Li, *ACS Biomater. Sci. Eng.*, 2022, **8**, 1749–1762.
100 D. Sharma, I. Dhiman, S. Das, D. K. Das, D. D. Pramanik, S. K. Dash and A. Pramanik, *ACS Omega*, 2025, **10**, 17087–17107.
101 W. Li, F. Separovic, N. M. O'Brien-Simpson and J. D. Wade, *Chem. Soc. Rev.*, 2021, **50**, 4932–4973.
102 Y. C. Chen, K. Y. A. Lin, C. C. Lin, T. Y. Lu, Y. H. Lin, C. H. Lin and K. F. Chen, *Photochem. Photobiol. Sci.*, 2019, **18**, 2442–2448.
103 N. A. Samak, M. S. Selim, Z. Hao and J. Xing, *J. Hazard. Mater.*, 2022, **426**, 128035.
104 X. Lu, J. Liu, L. Gou, J. Li, B. Yuan, K. Yang and Y. Ma, *Adv. Healthcare Mater.*, 2019, **8**, e1801521.
105 T. Lee, V. Hofferek, F. Separovic, G. E. Reid and M. Aguilar, *Curr. Opin. Chem. Biol.*, 2019, **52**, 85–92.
106 D. P. Singh, C. E. Herrera, B. Singh, S. Singh, R. K. Singh and R. Kumar, *Mater. Sci. Eng., C*, 2018, **86**, 173–197.
107 B. Vidmar, R. Marinsek Logar, M. Panjicko and L. Fanedl, *Acta Chim. Slov.*, 2017, **64**, 227–236.
108 C. Zhong, X. Hu, X. Yang, H. Gan, K. Yan, F. Shu, P. Wei, T. Gong, P. Luo, T. D. James, Z. Chen, Y. Zheng, X. He and Z. Xia, *ACS Appl. Mater. Interfaces*, 2022, **14**, 39808–39818.
109 H. A. Hemeg, *Z. Naturforsch., C: J. Biosci.*, 2022, **77**, 365–378.
110 S. U. Haq, W. Ling, A. I. Aqib, H. Danmei, M. T. Aleem, M. Fatima, S. Ahmad and F. Gao, *Eur. J. Pharmacol.*, 2025, **998**, 177511.